Neuron
Report

Regulation of Presynaptic Neurotransmission by Macroautophagy

Daniela Hernandez,[1,6] Ciara A. Torres,[2,6] Wanda Setlik,[3] Carolina Cebrián,[4] Eugene V. Mosharov,[4] Guomei Tang,[4] Hsiao-Chun Cheng,[4] Nikolai Kholodilov,[4] Olga Yarygina,[4] Robert E. Burke,[4] Michael Gershon,[3] and David Sulzer[4,5,*]
[1]Department of Neuroscience
[2]Integrated Program in Cellular, Molecular, and Biomedical Studies
[3]Department of Pathology
[4]Department of Neurology
[5]Department of Psychiatry and Pharmacology
Columbia University Medical Campus, New York, NY 10013, USA
[6]These authors contributed equally to this work
*Correspondence: ds43@columbia.edu
DOI 10.1016/j.neuron.2012.02.020

SUMMARY

mTOR is a regulator of cell growth and survival, protein synthesis-dependent synaptic plasticity, and autophagic degradation of cellular components. When triggered by mTOR inactivation, macroautophagy degrades long-lived proteins and organelles via sequestration into autophagic vacuoles. mTOR further regulates synaptic plasticity, and neurodegeneration occurs when macroautophagy is deficient. It is nevertheless unknown whether macroautophagy modulates presynaptic function. We find that the mTOR inhibitor rapamycin induces formation of autophagic vacuoles in prejunctional dopaminergic axons with associated decreased axonal profile volumes, synaptic vesicle numbers, and evoked dopamine release. Evoked dopamine secretion was enhanced and recovery was accelerated in transgenic mice in which macroautophagy deficiency was restricted to dopaminergic neurons; rapamycin failed to decrease evoked dopamine release in the striatum of these mice. Macroautophagy that follows mTOR inhibition in presynaptic terminals, therefore, rapidly alters presynaptic structure and neurotransmission.

INTRODUCTION

The kinase mammalian target of rapamycin (mTOR) regulates protein synthesis (Huang and Manning, 2009) and degradation (Cuervo, 2004). mTOR activity enhances protein synthesis via participation in the complex mTORC1, which phosphorylates S6, S6 kinase, and 4E-BP (Huang and Manning, 2009). mTORC1 also phosphorylates Atg13, inhibiting Atg1, which is required for the induction of macroautophagy (Kamada et al., 2010). mTOR activity, therefore, both enhances protein synthesis and inhibits cellular degradation pathways.

In the nervous system, mTORC1 activity stimulates protein synthesis-dependent synaptic plasticity and learning (Huang and Manning, 2009; Long et al., 2004; Richter and Klann, 2009). Most studies on cellular and neuronal functions of mTOR use rapamycin, an inhibitor that, when bound to FKBP12, interacts with mTOR's FRB domain and prevents mTOR from binding raptor, a component of the mTORC1 complex (Dowling et al., 2010). Rapamycin blocks axonal hyperexcitability and synaptic plasticity in cellular models of injury, as well as learning and memory, by inhibiting protein synthesis (Hu et al., 2007; Weragoda and Walters, 2007).

Macroautophagy is a highly conserved cellular degradative process in which proteins and organelles are engulfed by autophagic vacuoles (AVs) that are subsequently targeted for degradation in lysosomes. It is possible that degradation of pre- or postsynaptic components could contribute to plasticity: for example, local mTOR inhibition might elicit autophagic degradation of synaptic vesicles, providing a means of presynaptic depression. We therefore explored whether mTOR-regulated degradation of proteins and organelles via macroautophagy alters synaptic function and morphology.

To do so, we generated transgenic mice in which macroautophagy was selectively inactivated in dopamine neurons. These neurons are deficient in expression of Atg7, an E1-like enzyme that conjugates microtubule-associated protein light chain 3 (LC3) to phospholipid and Atg5 to Atg12, steps that are necessary for AV formation (Martinez-Vicente and Cuervo, 2007). We chose to specifically delete Atg7 to abolish macroautophagy and the formation of AVs because, in contrast to Atg1, it is not thought to directly regulate membrane trafficking (Wairkar et al., 2009).

We chose to examine presynaptic structure and function in the dopamine system because (1) in the acute striatal slice preparation, dopamine axons are severed from their cell bodies but continue to synthesize, release, and reaccumulate neurotransmitter for up to 10 hr, allowing us to clearly focus on axonal autophagy, and (2) electrochemical recordings of evoked dopamine release and reuptake in the striatum provide a unique means to measure central nervous system (CNS) neurotransmission with millisecond resolution that is independent of postsynaptic response.

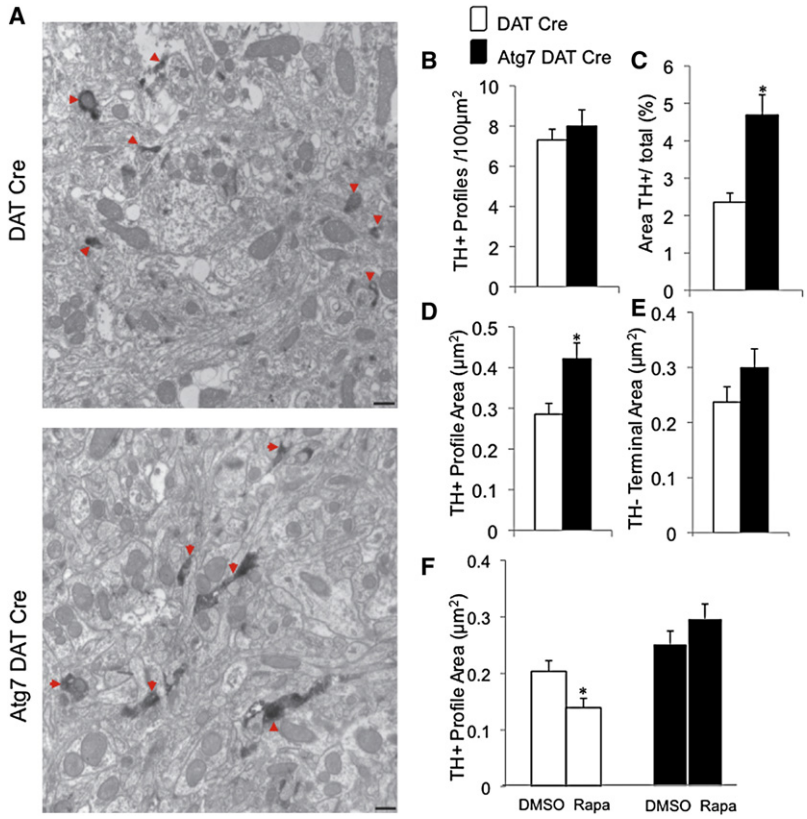

Figure 1. Macroautophagy Deficiency Results in Morphological Alterations In Vivo

Dopaminergic striatal axonal projections from 8-week-old male mice were identified by TH immunolabel. (A) Representative electron micrographs in DAT Cre and Atg7 DAT Cre mice. Arrowheads indicate TH^+ axonal profiles. Scale bars represent 500 nm. (B) There was no difference in the number of TH^+ profiles/100 μm^2 between DAT Cre and Atg7 DAT Cre mice ($p > 0.05$; t test). (C) The total area occupied by TH^+ profiles in striatum from Atg7 DAT Cre was larger than in DAT Cre mice ($p < 0.05$; two-tailed t test). (D) The average area of TH^+ profiles was 45% larger in Atg7 DAT Cre ($n = 84$) than DAT Cre ($n = 61$) ($p < 0.05$; t test). (E) There was no significant difference in the size of TH^- profiles between DAT Cre ($n = 26$) and Atg7 DAT Cre ($n = 27$) mice ($p > 0.05$; t test). (F) Rapamycin in vivo (administered twice, 36 and 12 hr prior to sacrifice) decreased TH^+ profiles by 32% in DAT Cre mice ($n = 51$, DMSO; $n = 54$, rapamycin), but not in Atg7 DAT Cre mice ($n = 116$, DMSO; $n = 61$, rapamycin; interaction between rapamycin and genotype, $F = 6.72$; $p < 0.01$; two-way ANOVA). Error bars indicate SEM.

We found that (1) chronic macroautophagy deficiency in dopamine neurons resulted in increased size of axon profiles, increased evoked dopamine release, and more rapid presynaptic recovery; (2) in mice with intact macroautophagy, mTOR inhibition with rapamycin acutely increased AV formation in axons, decreased the number of synaptic vesicles, and depressed evoked dopamine release; and (3) rapamycin had no effect on evoked dopamine release and synaptic vesicles in dopamine neuron-specific macroautophagy-deficient mice. We conclude that mTOR-dependent local axonal macroautophagy can rapidly regulate presynaptic structure and function.

RESULTS

Dopamine Neuron-Specific Autophagy-Deficient Mice

We generated dopamine neuron-specific macroautophagy-deficient mice by crossing $Atg7^{flox/flox}$ mice (Komatsu et al., 2005) to a line expressing Cre recombinase under the dopamine transporter (DAT) promoter (DAT Cre/+) (Zhuang et al., 2005). The progeny ($Atg7^{flox/+}$;DAT Cre/+) were crossed to $Atg7^{flox/flox}$ to generate $Atg7^{flox/flox}$;DAT Cre/+ (Atg7 DAT Cre). Because the mutant mice have a single functional copy of *DAT*, we used DAT Cre/+ (DAT Cre) animals as controls; these animals express two copies of wild-type *Atg7* and a single functional copy of *DAT*.

We detected *Atg7* expression by nonradioactive in situ hybridization using an RNA probe designed against nucleotides 1518–1860 of the *Atg7* gene in 8- to 10-week-old mice. *Atg7* mRNA was detected in both the anterior and central substantia nigra pars compacta and pars reticulata in DAT Cre animals but was absent in Atg7 DAT Cre mice. *Atg7* mRNA was detected in the red nucleus (RN) and in the dentate gyrus (DG) from Atg7 DAT Cre, further indicating cellular specificity for the knocked out gene (see Figure S1 available online). We conclude that the *Atg7* gene was effectively deleted in ventral midbrain dopamine neurons.

In contrast to CNS-wide macroautophagy-deficient mice, which are smaller than controls, exhibit abnormal limb clasping, and begin to die at 4 weeks (Hara et al., 2006; Komatsu et al., 2006), Atg7 DAT Cre mice showed similar survival and weight gain as DAT Cre mice at 8 weeks of age (mean weights: 22.7 ± 1.1 g and 25.2 ± 1.6 g, respectively; $p > 0.05$; $n = 6$ mice per group; t test). The limb-clasping reflex of Atg7 DAT Cre mice was normal (data not shown). To evaluate motor behavior in tasks thought to specifically involve dopamine transmission (Crawley, 1999; Karl et al., 2003), we performed tail-hang, beam-walk, and open-field tests on mice aged 6–12 weeks. Motor performances of Atg7 DAT Cre mice were not different than DAT Cre in any of the tests ($n = 4$ in each group; data not shown). We did not examine mice older than 3 months in this study, and motor and behavioral differences may develop in aged mice.

Dopaminergic Axonal Profiles Are Larger in the Autophagy-Deficient Mice

We examined striatal dopaminergic axonal profiles immunolabeled for tyrosine hydroxylase (TH) from 8-week-old DAT Cre and Atg7 DAT Cre mice by electron microscopy (Figure 1A). There was no difference in the number of striatal TH immunoreactive axonal profiles per area in Atg7 DAT Cre mice (Figure 1B). There was, however, an increase in the fraction of total area occupied by TH^+ profiles: TH^+ axon profiles occupied 2.3% ± 0.2% of the total sampled area in the striatum of DAT

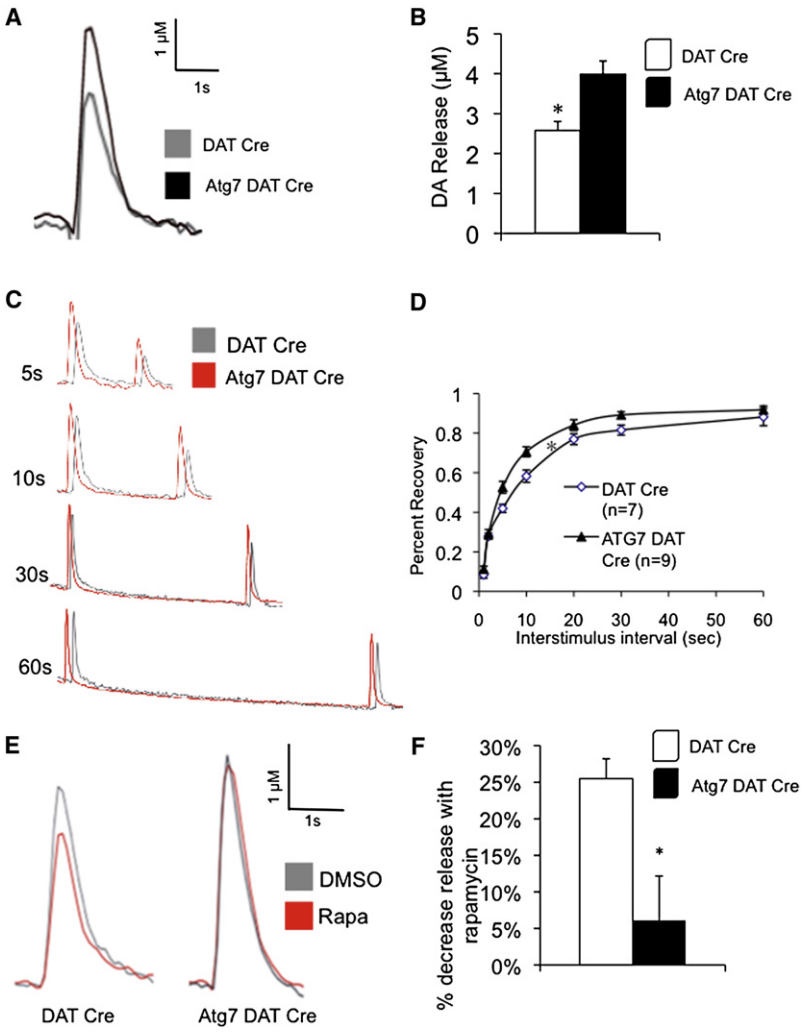

Figure 2. Evoked Dopamine Release in Atg7 DAT Cre Mice

(A) Cyclic voltammetry recordings of evoked dopamine release from slices of dorsal striatum from DAT Cre and Atg7 DAT Cre mice. (B) Evoked DA release was higher in Atg7 DAT Cre mice than in DAT Cre controls ($p < 0.005$; t test). There was no difference in the half-life ($t_{1/2}$) of the DA signals from DAT Cre and Atg7 DAT Cre (Figure S2). (C) Representative traces from paired-pulse recordings at interstimulus intervals of 5–60 s from a DAT Cre and Atg7 DAT Cre slice (slightly offset to aid comparison). (D) Paired-pulse ratio at interstimulus intervals of 1–60 s (mean ± SEM). Atg7 DAT Cre recovery was faster than DAT Cre controls ($p < 0.05$; repeated-measures ANOVA). (E) Representative traces from control (DMSO vehicle) and rapamycin-treated (red) DAT Cre and Atg7 DAT Cre slices. (F) Rapamycin decreased the peak amplitude of dopamine signals in DAT Cre striata by 25% ± 3% but decreased it by only 6% ± 6% in Atg7 DAT Cre striata ($p < 0.05$; two-way ANOVA). Rapamycin had no effect on the signal $t_{1/2}$ (Figure S2). Error bars indicate SEM.

Cre mice but 4.7% ± 0.5% of the area in Atg7 DAT Cre mice ($p < 0.005$; t test; >6,000 μm^2 sampled per condition in ten and eight micrographs, respectively; Figure 1C). Consistently, striatal TH^+ axonal profiles from Atg7 DAT Cre mice (0.42 ± 0.04 μm^2, n = 84) were larger than profiles from DAT Cre animals (0.29 ± 0.03 μm^2, n = 60; $p < 0.05$; Mann-Whitney test; Figure 1D). We found no difference in the size of terminals unlabeled for TH between DAT Cre and Atg7 DAT Cre mice (0.24 ± 0.03 μm^2, n = 26; 0.30 ± 0.03 μm^2, n = 27; $p > 0.05$; t test; Figure 1E).

To explore the effects of mTOR inhibition and macroautophagy deficiency on the size of dopamine axonal profiles, we injected pairs of DAT Cre and Atg7 DAT Cre mice with rapamycin (2 mg/kg) or vehicle (DMSO) 36 and 12 hr prior to perfusion. Rapamycin decreased the area of TH^+ striatal axon profiles by 32% in DAT Cre mice but had no effect on DA terminals of the DAT Cre Atg7 mutant line (Figure 1F) (interaction between rapamycin and genotype, $F = 6.72$; $p < 0.01$; two-way analysis of variance [ANOVA]).

Dopamine Neurotransmission in Atg7 DAT Cre Mice

We used cyclic voltammetry to directly measure evoked dopamine release and reuptake in the striatum. The peak amplitude of the signal is dependent on both neurosecretion and reuptake through DAT, whereas the half-life ($t_{1/2}$) is a function of DAT activity (Schmitz et al., 2001).

The amplitude of the dopamine signal evoked by a single pulse of electrical stimulation in Atg7 DAT Cre mice was 54% greater than in DAT Cre controls (n = 9 and n = 7, respectively; 4.0 ± 0.3 and 2.6 ± 0.2 nM, respectively; $p < 0.005$; t test; Figures 2A and 2B). As DAT Cre and Atg7 DAT Cre mice express a single functional copy of DAT, the signal duration in both genotypes was longer than in wild-type mice (mean $t_{1/2}$: ~490 ms) (Schmitz et al., 2001), but the mean $t_{1/2}$ of DAT signals from DAT Cre and Atg7 DAT Cre slices was not different (Figure S2A; mean $t_{1/2}$: 637 ± 51 and 662 ± 23 ms, respectively; $p > 0.05$; t test), which indicates that reuptake kinetics are similar and that the increased peak amplitude in the Atg7-deficient line was due to greater dopamine release rather than decreased reuptake.

To measure the rate of presynaptic recovery, we stimulated dopamine release with pairs of pulses separated by intervals that ranged from 1 to 60 s (Schmitz et al., 2002). Atg7 DAT Cre mice exhibited faster recovery ($p < 0.05$; repeated-measures ANOVA; Figure 2D), suggesting that basal macroautophagy can restrict synaptic transmission.

We then examined effects of rapamycin on evoked dopamine release. Striatal slices were bisected, and one striatum was exposed to rapamycin (3 μM, >5.5 hr)and the other to vehicle. Rapamycin decreased dopamine release evoked by a single electrical stimulus by 25% ± 3% in DAT Cre slices (n = 7) and by 6% ± 6% in Atg7 DAT Cre slices (n = 9; $p < 0.05$; two-way ANOVA; Newman-Keuls posttest; Figures 2E and 2F). Rapamycin did not significantly alter the $t_{1/2}$ of the signals from DAT Cre (control: 718 ± 29 ms; Rapa: 675 ± 22 ms) or Atg7 DAT Cre

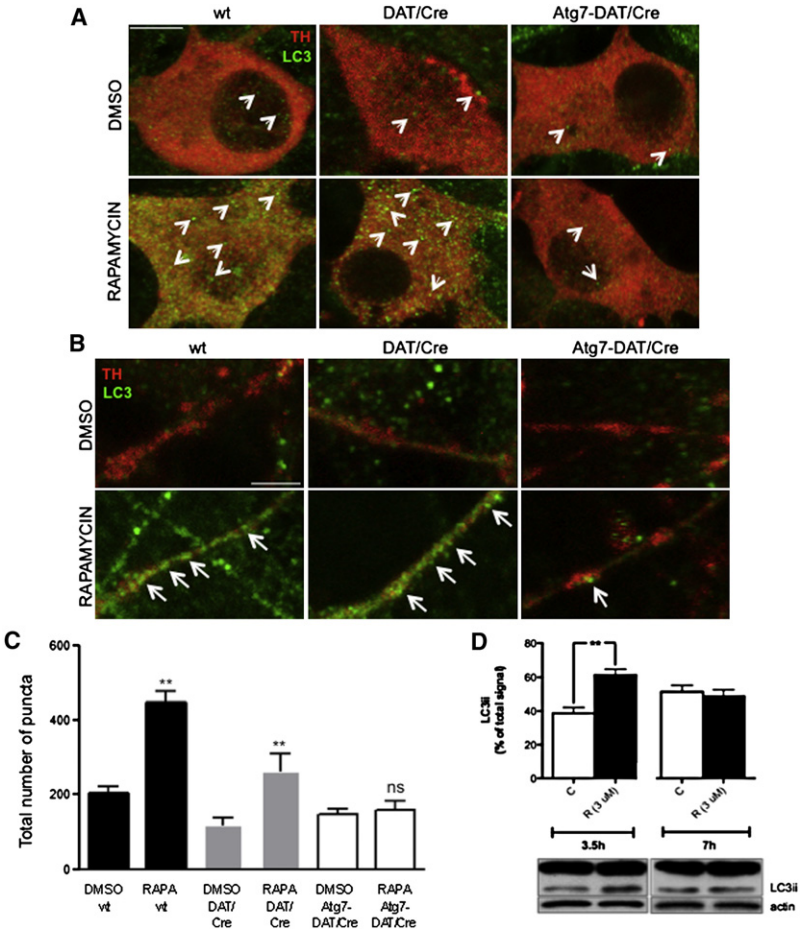

Figure 3. Rapamycin Effects on LC3 in VM DA Neurons

(A) Somatodendritic regions of dopaminergic neurons (TH^+, red immunolabel) derived from wild-type (WT) and DAT Cre mice exposed to rapamycin (RAPA, 3 μM, 3.5 hr) exhibited an increased number of LC3+ puncta (green immunolabel, examples indicated by white arrowheads) compared to dopaminergic neurons treated with vehicle (DMSO). There was no induction of LC3+ puncta by rapamycin in DA neurons from Atg7 DAT Cre mice. Scale bar represents 10 μm. (B) Similar results were observed throughout neurites. Rapamycin increased LC3 puncta (white arrows) in TH^+ neurites, but not in Atg7-deficient dopaminergic neurites. Scale bar represents 4 μm. (C) Number of LC3+ puncta per TH^+ neuron (cell bodies and neurites) for these conditions (mean ± SEM; n = 3 experimental repeats, 30 neurons rated per experiment per condition; t test; ns, nonsignificant; $^{**}p < 0.01$). (D) Rapamycin at 3.5 hr increased LC3-II by 56% (n = 3; $p < 0.001$; two-way ANOVA) but had no effect at 7 hr, indicating a temporary induction of LC-II in the slice preparation consistent with turnover of AVs. Error bars indicate SEM.

(control: 753 ± 23 ms; Rapa: 743 ± 32 ms) mice (Figure S2A; $p > 0.05$; two-way ANOVA).

The data indicate that the bulk of rapamycin's inhibition of evoked dopamine release is mediated by macroautophagy. To confirm that these effects were not limited to DAT Cre mutants, we repeated the recordings in slices from wild-type mice and observed a similar rapamycin-induced reduction in dopamine secretion (Figure S2B).

Effects of Acute Rapamycin Treatment

To examine the effect of acute mTOR inhibition on AV formation, we first exposed postnatally derived ventral midbrain neuronal cultures (Rayport et al., 1992) to rapamycin (200 nM, 3.5 hr). The macroautophagy-related protein LC3 exists in two forms, LC3-I and LC3-II, a phosphatidylethanolamine-conjugated form of LC3-I. LC3-I is widely distributed in the cytosol, whereas the conjugated LC3-II form specifically associates with AV membranes (Mizushima et al., 2004). Dopamine neurons were identified by TH immunolabel, and immunolabel for native LC3 was used to identify AVs. There were occasional LC3-immunolabeled puncta in the Atg7-deficient cell bodies and neurites, possibly due to noncanonical AV formation (Nishida et al., 2009). Rapamycin strikingly increased LC3-immunolabeled puncta in dopamine cell bodies and neurites in DAT Cre mice but had no effect on puncta in DAT Cre Atg7 mutants ($p < 0.01$; ANOVA) (Figures 3A–3C), showing that induction of AVs by rapamycin required Atg7 expression.

We then examined the induction of LC3-II by rapamycin (3 μM) in acute striatal slices by western blotting. Rapamycin at 3.5 hr produced a 56% increase in LC3-II (Figure 3D) ($p < 0.001$; t test), but this response was no longer apparent at 7 hr, indicating that rapamycin induced a transient increase of LC3-II, a characteristic of macroautophagy.

In electron micrographs of striatal slices, we identified AV-like organelles based on previously described criteria (Yu et al., 2004) as nonmitochondrial structures in presynaptic terminals that possessed multiple membranes, usually with luminal content. These organelles were different from multivesicular bodies, organelles of the autophagic-lysosomal pathway that typically displays an even distribution of vesicles in the lumen. Many AV-like organelles contained a wide range of luminal constituents, including small vesicles resembling synaptic vesicles (compare Figures 4A and 4B). Some multilamellar structures were devoid of obvious luminal electron-dense material (Martinez-Vicente et al., 2010), possibly due to acute induction of AVs by rapamycin. It is likely that some of these multilamellar organelles include endosomes or are "amphisomes" that result from fusion of endosomes and AVs. Rapamycin in the striatal slice more than doubled the number of presynaptic terminal profiles containing AV-like structures from 15.4% of control terminal profiles (n = 65) to 35.5% in rapamycin-treated terminals (n = 75; $p < 0.05$; chi-square test; Figure 4C) and decreased terminal profile areas by 19% ($p < 0.05$; t test; Figure 4D). Striatal terminal profiles from rapamycin-treated samples, of which only a small fraction are dopaminergic, moreover contained fewer synaptic vesicles than untreated controls (49.2 ± 3.6, n = 75 versus 70.1 ± 4.2, n = 65; $p < 0.0001$, respectively; t test; Figure 4E).

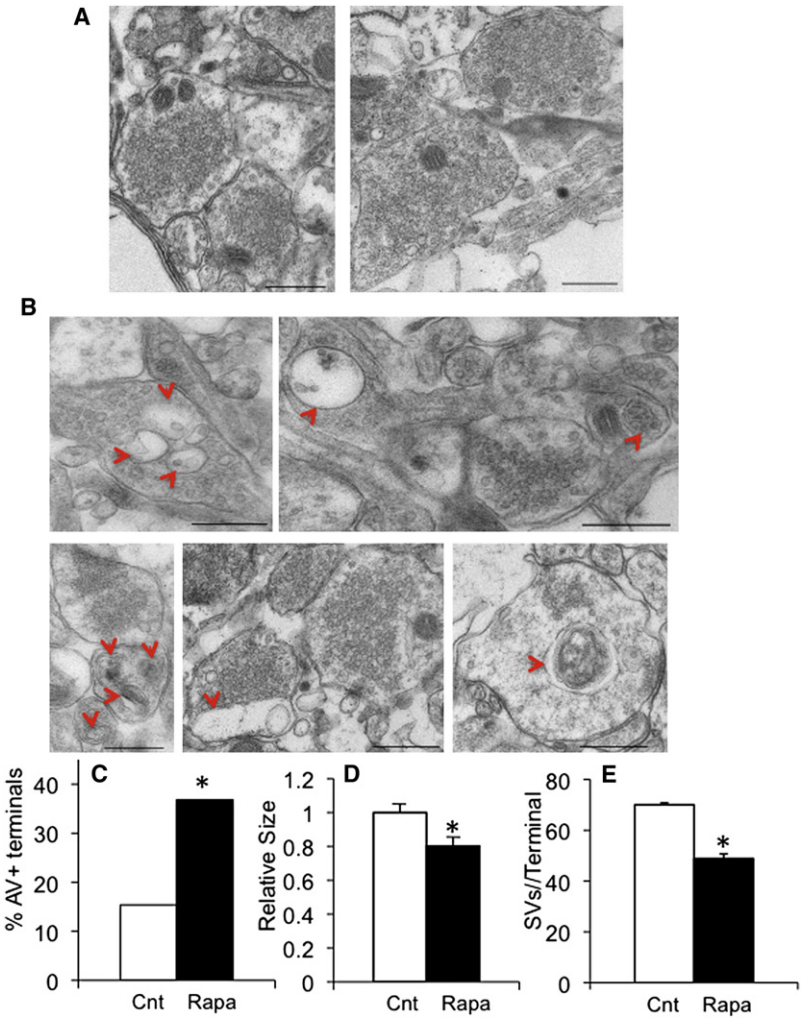

Figure 4. Acute mTOR Inhibition Induces Morphological Changes at Synaptic Terminal Profiles

(A and B) Electron micrographs from untreated corticostriatal slices (A) and rapamycin-treated corticostriatal slices (3 μM, 7 hr) (B). Presynaptic terminal AV-like organelles are marked by red arrowheads. Scale bars represent 500 nm. (C) Rapamycin increased the fraction of synaptic terminal profiles with AV-like organelles ($p < 0.05$; chi-square). (D) Acute rapamycin decreased terminal profile area ($p < 0.05$; t test). (E) Synaptic terminal profiles from rapamycin-treated slices contained fewer synaptic vesicles than untreated slices ($p < 0.0001$; t test). Error bars indicate SEM.

Dopamine axonal varicosities typically do not display presynaptic or postsynaptic densities (Nirenberg et al., 1997), but amperometric studies demonstrate stimulation-evoked quantal transmitter release from these structures (Pothos et al., 1998), and many accumulate and secrete fluorescent dopamine analogs (Gubernator et al., 2009), confirming their identity as presynaptic terminals. Because TH immunolabel obscured synaptic vesicles and other intracellular structures (see Figure 1), we examined whether rapamycin reduced the number of dopaminergic synaptic vesicles by using the false neurotransmitter 5-hydroxydopamine (5OHDA), which is selectively accumulated into these dopaminergic synaptic vesicles and produces osmophilic dense cores (Tennyson et al., 1974) (Figure 5, blue arrows). For each experiment, striatal slices were obtained from a single mouse, bisected, and individual striata were incubated in vehicle (DMSO) or rapamycin (3 μM, 6.5 hr) and then treated with 5OHDA (500 μM, 30 min). The numbers of synaptic vesicles in the labeled terminals were compared between slices derived from the same mouse. In a wild-type mouse, rapamycin decreased synaptic vesicles within 5OHDA-labeled terminals by 18% (from 105 to 86 synaptic vesicles per μm^2; $p < 0.02$; t test; 37 and 42 terminals rated), and in a DAT Cre mouse, rapamycin decreased synaptic vesicles within labeled terminals by 26% (from 82 to 61 synaptic vesicles per μm^2; $p = 0.05$; t test; 31 and 27 terminals rated). In contrast, rapamycin did not decrease synaptic vesicles within labeled terminals of an Atg7 DAT Cre mouse (84 to 95 synaptic vesicles per μm^2; $p = 0.13$; t test; 38 and 39 terminals rated), indicating that rapamycin decreased the number of dopaminergic synaptic vesicles only if Atg7 was present.

We compared the levels of a range of synaptic proteins between striatal slices of DAT Cre mice and Atg7 DAT Cre mice exposed to rapamycin (3 μM) or vehicle for 7 hr. Treated and untreated Atg7 DAT Cre mice showed substantially lower levels of DAT (Figure S3; Table S1), a small but significant decrease of TH ($p < 0.05$; two-factor ANOVA), similar levels ($p > 0.5$) of the postsynaptic marker PSD95, and the mitochondrial proteins porin, tomm20, and tim23. Although there was a transient increase in LC3-II at 3.5 hr (Figure 3D), no protein examined was altered by rapamycin at 7 hr. It may be that although this period provided sequestration of cellular elements in AVs, there was no measurable net degradation over this period. Note that only axons of dopamine neurons were present, and corresponding cell bodies with mature lysosomes were absent.

DISCUSSION

Our data indicate that both basal and induced macroautophagy modulates presynaptic structure and function. Mice with chronic macroautophagy deficiency in dopamine neurons had abnormally large dopaminergic axonal profiles, released greater levels of neurotransmitter in response to stimulation, and exhibited more rapid presynaptic recovery. mTOR inhibition by rapamycin administered to control mice induced AV-like structures in axons and decreased synaptic vesicles to nearly the same level as the accompanying decrease in evoked dopamine release. In contrast, rapamycin had little or no effect on the number of synaptic vesicles or neurotransmitter release in

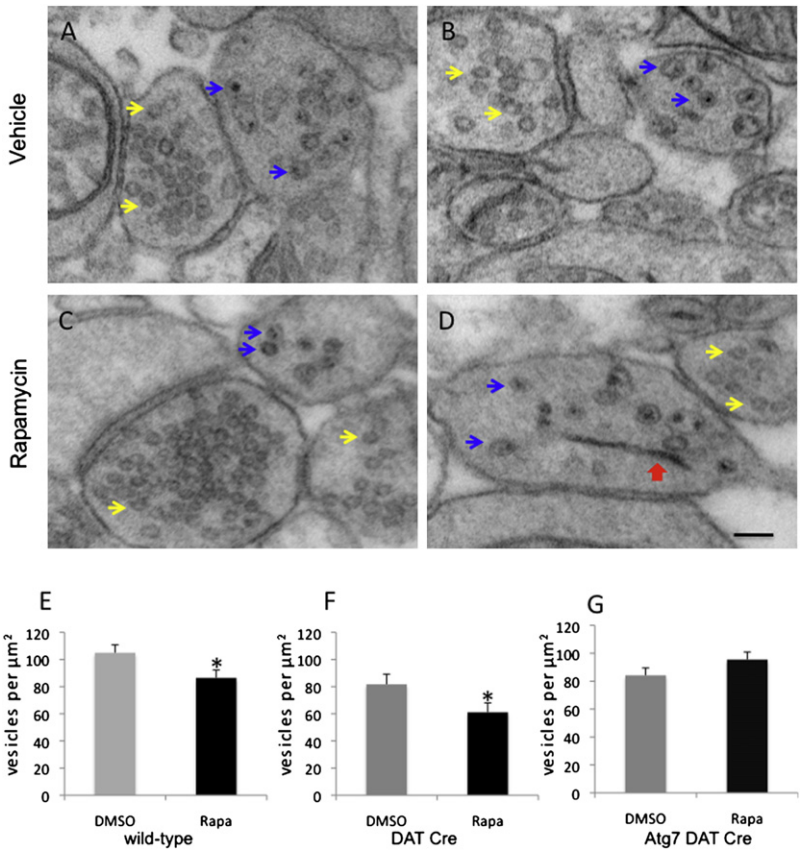

Figure 5. Effects of Rapamycin on Synaptic Vesicles in Terminals Labeled by the False Transmitter 5-Hydroxydopamine

For each experiment, slices from the same mouse were compared. (A and B) Examples of synaptic terminals from striatal slices from a wild-type mouse incubated with vehicle (DMSO) for 6.5 hr and followed by 5-hydroxydopamine (5OHDA) (500 μM) for 30 min. (C and D) Examples of terminals in the striatal slice exposed to rapamycin (3 μM, 6.5 hr) and followed by 5OHDA for 30 min. Yellow arrows indicate examples of synaptic vesicles in nondopaminergic terminals; blue arrows indicate labeled dopaminergic synaptic vesicles; red arrow indicates a structure that may be an isolation membrane. Scale bar represents 100 nm. (E–G) Number of synaptic vesicles per unit area (μm^2) of 5OHDA-labeled terminals after exposure to DMSO or rapamycin in wild-type (E), DAT Cre (F), or Atg7 DAT Cre (G) striatal slices. *$p < 0.05$; t test. Error bars indicate SEM.

macroautophagy-deficient neurons. Together, our results introduce acute presynaptic changes that depend on Atg7 expression and hence macroautophagy.

These presynaptic effects were observed in dopaminergic presynaptic terminals in slices without their cell bodies, and so the critical steps in autophagy must have occurred locally in axons that typically lack mature lysosomes (Overly et al., 1995). Our data confirm that AVs can be synthesized locally in the axons (Lee et al., 2011) and indicate that local axonal autophagy can sequester presynaptic components and modulate presynaptic function. This evidence extends studies of selective degradation of postsynaptic receptors via macroautophagy (Hanley, 2010; Matsuda et al., 2008; Rowland et al., 2006) and classic work indicating a role for lysosomal degradation in recycling synaptic vesicle turnover (Holtzman et al., 1971). Thus, in addition to well-established roles of macroautophagy in stress response and cellular homeostasis (Tooze and Schiavo, 2008), neurons have adapted this phylogenetically ancient process to modulate neurotransmitter release and remodel synapses.

Chronic Macroautophagy Deficiency and Neuronal Morphology

Macroautophagy deficiency throughout the CNS results in decreased weight, motor deficits, and premature death (Hara et al., 2006; Komatsu et al., 2006). Purkinje cells from cell-specific autophagy-deficient mice show axonal swellings and signs of neurodegeneration as early as postnatal day 19 (Komatsu et al., 2007). Signs of neurodegeneration were, however, not observed in young DAT Cre Atg7 mice (<14 weeks), possibly due to compensation by other degradative pathways (Koga et al., 2011). It may be that further aged DAT Cre Atg7 mice model aspects of Parkinson's-related disorders.

Chronic autophagy deficiency rather increased the size of dopaminergic synaptic terminal profiles and striatal dopaminergic innervation, consistent with studies that implicate macroautophagy in retraction of neuronal processes (Bunge, 1973) and neuritic growth in developing neurons (Hollenbeck, 1993). The results, however, contrast with studies in *Drosophila*, in which disruption of AV formation or AV-lysosomal fusion decreases the size of the neuromuscular junction, whereas Atg1 overexpression or rapamycin promotes macroautophagy and increases the number of synaptic boutons and neuritic branches (Shen and Ganetzky, 2009). Some synaptic Atg1-related changes may be autophagy independent because the loss of other autophagy-related proteins does not mimic the effect of Atg1 overexpression on the number of boutons and neurite branches (Toda et al., 2008; Wairkar et al., 2009).

We further observed that chronic Atg7 deficiency in dopamine terminals led to an increase in presynaptic mitochondria (data not shown); Atg7 deficiency may contribute to changes in mitochondria in multiple ways, for example, via effects on presynaptic mitochondria size, shape, trafficking, fission, and fusion.

Autophagy Induction and Synaptic Vesicles

Acute induction of AVs by rapamycin in control neurons was confirmed by electron microscopy, LC3 immunolabel, and transiently elevated LC3-II. Acute exposure to rapamycin decreased synaptic terminal profile size and number of synaptic vesicles, indicating that mTOR inhibition can rapidly decrease presynaptic components. Some AV-like profiles contained cargo that resembled synaptic vesicles, although we were unable to immunolabel AV components, presumably due to the low luminal

pH. Presynaptic terminals are very active in endocytosis due to the turnover and recycling of synaptic vesicles, receptors, and other constituents, and it is likely that many of the multilamellar organelles we observe are products of the fusion of endosomes and AVs, sometimes called "amphisomes." An apparently clear content of occasional AV-like organelles suggests that acute mTOR blockade may result in some "empty" early AVs (Martinez-Vicente et al., 2010).

AV-like profiles were absent in dopamine axon profiles of the Atg7-deficient mice, and although low levels of LC3-immunolabeled puncta were present in the mutant neurons, they were not enhanced by rapamycin. Thus, the increase in AVs by mTOR inhibition apparently requires Atg7, and we hypothesize that, in normal neurons, rapamycin redistributed synaptic vesicle membranes into axonal AVs, endosomes, and/or amphisomes.

Synaptic Transmission in Atg7 DAT Cre Animals

Chronic lack of macroautophagy enhanced evoked dopamine release and the rate of synaptic recovery. At a variety of synapses, a higher release probability can increase the peak amplitude from the first pulse followed by a relative depression from the second pulse, due to a decreased availability of release-ready vesicles, culminating in a lower paired-pulse ratio (second pulse/first pulse). This situation differs from that in Atg7 DAT Cre animals, in which both the initial and subsequent pulses showed increased amplitudes relative to control mice. The probability of dopaminergic synaptic vesicle fusion is regulated by the size of the recycling and readily releasable pools (Daniel et al., 2009): the enhanced release and recovery in the mutant line could be due to multiple nonexclusive effects, including a greater synaptic terminal size or density, a greater number of synaptic vesicles, more calcium influx, or an increase in vesicle docking and fusion sites and/or rates. We measured lower total striatal DAT and TH levels in the macroautophagy-deficient line, although the kinetics of dopamine release do not indicate altered activity of the proteins, which are regulated by a variety of compensatory mechanisms (Schmitz et al., 2003).

Rapamycin depressed evoked dopamine release in control mice but had no effect in Atg7 DAT Cre mice, confirming that the rapid changes in neurotransmission evoked by mTOR inhibtion were macroautophagy dependent and not the result of effects on protein synthesis.

Although we have focused on dopaminergic terminals, the data suggest that these effects are not specific to them. Rapamycin induced apparent AVs in both dopaminergic (TH^+) and nondopaminergic (TH^-) terminals, and a decrease in synaptic vesicles was observed generally in striatal synaptic terminals, which include glutamatergic, dopaminergic, GABAergic, and cholinergic synaptic terminals. Our experiments do not address how subsets of particular presynaptic organelles, such as individual synaptic vesicles, may be specifically targeted by mTOR-dependent axonal macroautophagy. Clues might be offered if alternative modes of vesicle recycling are identified that could partake in or avoid endocytic compartments that might fuse with AVs (Voglmaier et al., 2006).

Starvation, injury, oxidative stress, toxins, including methamphetamine, and infection by neurotropic viruses trigger autophagy in neurons, which is further associated with protein aggregate-related disorders, including Huntington's, Parkinson's, and Alzheimer's diseases (Cheng et al., 2011; Koga et al., 2011; Larsen et al., 2002; Tallóczy et al., 2002; Tooze and Schiavo, 2008). mTOR activity is regulated by multiple endogenous pathways involved in synaptic activity and stress, including tuberous sclerosis complex, Rheb, AKT, NF1, and PTEN (Malagelada et al., 2010). Alterations in mTOR activity are associated with neuropathological conditions such as epilepsy, tuberous sclerosis, and autism. Regulation of presynaptic function by mTOR activity and macroautophagy could thus contribute to manifestations of neurological disorders.

EXPERIMENTAL PROCEDURES

Details of the experimental procedures can be found in the Supplemental Experimental Procedures.

SUPPLEMENTAL INFORMATION

Supplemental Information includes three figures, one table, and Supplemental Experimental Procedures and can be found with this article online at doi:10.1016/j.neuron.2012.02.020.

ACKNOWLEDGMENTS

We thank Ana Maria Cuervo, Zsolt Tallóczy, and Steven Siegelbaum for discussion. We thank Maksaaki Komatsu for providing the floxed Atg7 line. This work was funded by Udall Center of Excellence for Parkinson's Disease Research, NIH DA07418 and DA10154, the Parkinson's Disease Foundation, and the Picower Foundation.

Accepted: February 1, 2012
Published: April 25, 2012

REFERENCES

Bunge, M.B. (1973). Fine structure of nerve fibers and growth cones of isolated sympathetic neurons in culture. J. Cell Biol. *56*, 713–735.

Cheng, H.C., Kim, S.R., Oo, T.F., Kareva, T., Yarygina, O., Rzhetskaya, M., Wang, C., During, M., Talloczy, Z., Tanaka, K., et al. (2011). Akt suppresses retrograde degeneration of dopaminergic axons by inhibition of macroautophagy. J. Neurosci. *31*, 2125–2135.

Crawley, J.N. (1999). Behavioral phenotyping of transgenic and knockout mice: experimental design and evaluation of general health, sensory functions, motor abilities, and specific behavioral tests. Brain Res. *835*, 18–26.

Cuervo, A.M. (2004). Autophagy: many paths to the same end. Mol. Cell. Biochem. *263*, 55–72.

Daniel, J.A., Galbraith, S., Iacovitti, L., Abdipranoto, A., and Vissel, B. (2009). Functional heterogeneity at dopamine release sites. J. Neurosci. *29*, 14670–14680.

Dowling, R.J., Topisirovic, I., Fonseca, B.D., and Sonenberg, N. (2010). Dissecting the role of mTOR: lessons from mTOR inhibitors. Biochim Biophys Acta. *1804*, 433–439.

Gubernator, N.G., Zhang, H., Staal, R.G., Mosharov, E.V., Pereira, D.B., Yue, M., Balsanek, V., Vadola, P.A., Mukherjee, B., Edwards, R.H., et al. (2009). Fluorescent false neurotransmitters visualize dopamine release from individual presynaptic terminals. Science *324*, 1441–1444.

Hanley, J.G. (2010). Endosomal sorting of AMPA receptors in hippocampal neurons. Biochem. Soc. Trans. *38*, 460–465.

Hara, T., Nakamura, K., Matsui, M., Yamamoto, A., Nakahara, Y., Suzuki-Migishima, R., Yokoyama, M., Mishima, K., Saito, I., Okano, H., and Mizushima, N. (2006). Suppression of basal autophagy in neural cells causes neurodegenerative disease in mice. Nature *441*, 885–889.

Hollenbeck, P.J. (1993). Products of endocytosis and autophagy are retrieved from axons by regulated retrograde organelle transport. J. Cell Biol. *121*, 305–315.

Holtzman, E., Freeman, A.R., and Kashner, L.A. (1971). Stimulation-dependent alterations in peroxidase uptake at lobster neuromuscular junctions. Science *173*, 733–736.

Hu, J.Y., Chen, Y., and Schacher, S. (2007). Protein kinase C regulates local synthesis and secretion of a neuropeptide required for activity-dependent long-term synaptic plasticity. J. Neurosci. *27*, 8927–8939.

Huang, J., and Manning, B.D. (2009). A complex interplay between Akt, TSC2 and the two mTOR complexes. Biochem. Soc. Trans. *37*, 217–222.

Kamada, Y., Yoshino, K., Kondo, C., Kawamata, T., Oshiro, N., Yonezawa, K., and Ohsumi, Y. (2010). Tor directly controls the Atg1 kinase complex to regulate autophagy. Mol. Cell. Biol. *30*, 1049–1058.

Karl, T., Pabst, R., and von Hörsten, S. (2003). Behavioral phenotyping of mice in pharmacological and toxicological research. Exp. Toxicol. Pathol. *55*, 69–83.

Koga, H., Martinez-Vicente, M., Arias, E., Kaushik, S., Sulzer, D., and Cuervo, A.M. (2011). Constitutive upregulation of chaperone-mediated autophagy in Huntington's disease. J. Neurosci. *31*, 18492–18505.

Komatsu, M., Waguri, S., Ueno, T., Iwata, J., Murata, S., Tanida, I., Ezaki, J., Mizushima, N., Ohsumi, Y., Uchiyama, Y., et al. (2005). Impairment of starvation-induced and constitutive autophagy in Atg7-deficient mice. J. Cell Biol. *169*, 425–434.

Komatsu, M., Waguri, S., Chiba, T., Murata, S., Iwata, J., Tanida, I., Ueno, T., Koike, M., Uchiyama, Y., Kominami, E., and Tanaka, K. (2006). Loss of autophagy in the central nervous system causes neurodegeneration in mice. Nature *441*, 880–884.

Komatsu, M., Wang, Q.J., Holstein, G.R., Friedrich, V.L., Jr., Iwata, J., Kominami, E., Chait, B.T., Tanaka, K., and Yue, Z. (2007). Essential role for autophagy protein Atg7 in the maintenance of axonal homeostasis and the prevention of axonal degeneration. Proc. Natl. Acad. Sci. USA *104*, 14489–14494.

Larsen, K.E., Fon, E.A., Hastings, T.G., Edwards, R.H., and Sulzer, D. (2002). Methamphetamine-induced degeneration of dopaminergic neurons involves autophagy and upregulation of dopamine synthesis. J. Neurosci. *22*, 8951–8960.

Lee, S., Sato, Y., and Nixon, R.A. (2011). Lysosomal proteolysis inhibition selectively disrupts axonal transport of degradative organelles and causes an Alzheimer's-like axonal dystrophy. J. Neurosci. *31*, 7817–7830.

Long, X., Müller, F., and Avruch, J. (2004). TOR action in mammalian cells and in Caenorhabditis elegans. Curr. Top. Microbiol. Immunol. *279*, 115–138.

Malagelada, C., Jin, Z.H., Jackson-Lewis, V., Przedborski, S., and Greene, L.A. (2010). Rapamycin protects against neuron death in in vitro and in vivo models of Parkinson's disease. J. Neurosci. *30*, 1166–1175.

Martinez-Vicente, M., and Cuervo, A.M. (2007). Autophagy and neurodegeneration: when the cleaning crew goes on strike. Lancet Neurol. *6*, 352–361.

Martinez-Vicente, M., Talloczy, Z., Wong, E., Tang, G., Koga, H., Kaushik, S., de Vries, R., Arias, E., Harris, S., Sulzer, D., and Cuervo, A.M. (2010). Cargo recognition failure is responsible for inefficient autophagy in Huntington's disease. Nat. Neurosci. *13*, 567–576.

Matsuda, S., Miura, E., Matsuda, K., Kakegawa, W., Kohda, K., Watanabe, M., and Yuzaki, M. (2008). Accumulation of AMPA receptors in autophagosomes in neuronal axons lacking adaptor protein AP-4. Neuron *57*, 730–745.

Mizushima, N., Yamamoto, A., Matsui, M., Yoshimori, T., and Ohsumi, Y. (2004). In vivo analysis of autophagy in response to nutrient starvation using transgenic mice expressing a fluorescent autophagosome marker. Mol. Biol. Cell *15*, 1101–1111.

Nirenberg, M.J., Chan, J., Liu, Y., Edwards, R.H., and Pickel, V.M. (1997). Vesicular monoamine transporter-2: immunogold localization in striatal axons and terminals. Synapse *26*, 194–198.

Nishida, Y., Arakawa, S., Fujitani, K., Yamaguchi, H., Mizuta, T., Kanaseki, T., Komatsu, M., Otsu, K., Tsujimoto, Y., and Shimizu, S. (2009). Discovery of Atg5/Atg7-independent alternative macroautophagy. Nature *461*, 654–658.

Overly, C.C., Lee, K.D., Berthiaume, E., and Hollenbeck, P.J. (1995). Quantitative measurement of intraorganelle pH in the endosomal-lysosomal pathway in neurons by using ratiometric imaging with pyranine. Proc. Natl. Acad. Sci. USA *92*, 3156–3160.

Pothos, E.N., Davila, V., and Sulzer, D. (1998). Presynaptic recording of quanta from midbrain dopamine neurons and modulation of the quantal size. J. Neurosci. *18*, 4106–4118.

Rayport, S., Sulzer, D., Shi, W.X., Sawasdikosol, S., Monaco, J., Batson, D., and Rajendran, G. (1992). Identified postnatal mesolimbic dopamine neurons in culture: morphology and electrophysiology. J. Neurosci. *12*, 4264–4280.

Richter, J.D., and Klann, E. (2009). Making synaptic plasticity and memory last: mechanisms of translational regulation. Genes Dev. *23*, 1–11.

Rowland, A.M., Richmond, J.E., Olsen, J.G., Hall, D.H., and Bamber, B.A. (2006). Presynaptic terminals independently regulate synaptic clustering and autophagy of GABAA receptors in Caenorhabditis elegans. J. Neurosci. *26*, 1711–1720.

Schmitz, Y., Lee, C.J., Schmauss, C., Gonon, F., and Sulzer, D. (2001). Amphetamine distorts stimulation-dependent dopamine overflow: effects on D2 autoreceptors, transporters, and synaptic vesicle stores. J. Neurosci. *21*, 5916–5924.

Schmitz, Y., Schmauss, C., and Sulzer, D. (2002). Altered dopamine release and uptake kinetics in mice lacking D2 receptors. J. Neurosci. *22*, 8002–8009.

Schmitz, Y., Benoit-Marand, M., Gonon, F., and Sulzer, D. (2003). Presynaptic regulation of dopaminergic neurotransmission. J. Neurochem. *87*, 273–289.

Shen, W., and Ganetzky, B. (2009). Autophagy promotes synapse development in Drosophila. J. Cell Biol. *187*, 71–79.

Tallóczy, Z., Jiang, W., Virgin, H.W., 4th, Leib, D.A., Scheuner, D., Kaufman, R.J., Eskelinen, E.L., and Levine, B. (2002). Regulation of starvation- and virus-induced autophagy by the eIF2alpha kinase signaling pathway. Proc. Natl. Acad. Sci. USA *99*, 190–195.

Tennyson, V.M., Heikkila, R., Mytilineou, C., Côté, L., and Cohen, G. (1974). 5-Hydroxydopamine 'tagged' neuronal boutons in rabbit neostriatum: interrelationship between vesicles and axonal membrane. Brain Res. *82*, 341–348.

Toda, H., Mochizuki, H., Flores, R., 3rd, Josowitz, R., Krasieva, T.B., Lamorte, V.J., Suzuki, E., Gindhart, J.G., Furukubo-Tokunaga, K., and Tomoda, T. (2008). UNC-51/ATG1 kinase regulates axonal transport by mediating motor-cargo assembly. Genes Dev. *22*, 3292–3307.

Tooze, S.A., and Schiavo, G. (2008). Liaisons dangereuses: autophagy, neuronal survival and neurodegeneration. Curr. Opin. Neurobiol. *18*, 504–515.

Voglmaier, S.M., Kam, K., Yang, H., Fortin, D.L., Hua, Z., Nicoll, R.A., and Edwards, R.H. (2006). Distinct endocytic pathways control the rate and extent of synaptic vesicle protein recycling. Neuron *51*, 71–84.

Wairkar, Y.P., Toda, H., Mochizuki, H., Furukubo-Tokunaga, K., Tomoda, T., and Diantonio, A. (2009). Unc-51 controls active zone density and protein composition by downregulating ERK signaling. J. Neurosci. *29*, 517–528.

Weragoda, R.M., and Walters, E.T. (2007). Serotonin induces memory-like, rapamycin-sensitive hyperexcitability in sensory axons of aplysia that contributes to injury responses. J. Neurophysiol. *98*, 1231–1239.

Yu, W.H., Kumar, A., Peterhoff, C., Shapiro Kulnane, L., Uchiyama, Y., Lamb, B.T., Cuervo, A.M., and Nixon, R.A. (2004). Autophagic vacuoles are enriched in amyloid precursor protein-secretase activities: implications for beta-amyloid peptide over-production and localization in Alzheimer's disease. Int. J. Biochem. Cell Biol. *36*, 2531–2540.

Zhuang, X., Masson, J., Gingrich, J.A., Rayport, S., and Hen, R. (2005). Targeted gene expression in dopamine and serotonin neurons of the mouse brain. J. Neurosci. Methods *143*, 27–32.